Morphological and biochemical magnetic resonance techniques for cartilage imaging in rheumatoid arthritis: application and analysis

This article focuses on high-field (3.0 Tesla) MRI in the visualization of the small joints of the finger in rheumatoid arthritis. High spatial resolution, based on optimized coil equipment and advanced sequence protocols can be achieved for morphological and biochemical imaging of small structures in small joints. Besides the structural degradation, as visualized by advanced high-resolution morphological MRI, biochemical changes in the structure of articular cartilage can be imaged. Early proteoglycan loss, as well as changes in the collagen matrix, can be quantified using delayed gadolinium-enhanced MRI of cartilage and T2 mapping. Hence, using an advanced morphological and biochemical magnetic resonance protocol, the pathophysiological pathway of rheumatoid arthritis might be elucidated, providing an objective and quantitative method to monitoring disease progression.

KEYWORDS: articular cartilage ■ dGEMRIC ■ MRI ■ rheumatoid arthritis ■ T2 mapping

Goetz H Welsch[†1,2], Siegfried Trattnig[2], Nina Renner[1], Lars Lauer[3], Dominik Paul[3], Michael Uder[4], Philipp Schlechtweg[4], Rolf Janka[4] & Georg Schett[5]

[1]Department of Trauma Surgery, University of Erlangen-Nuremberg, Krankenhausstr. 12, 91054 Erlangen, Germany
[2]MR Center – High Field MR, Department of Radiology, Medical University of Vienna, Währinger Gürtel 18–20, A-1090 Vienna, Austria
[3]Siemens Healthcare, Alle Am Röthelheimpark 2, 91052 Erlangen, Germany
[4]Department of Radiology, University of Erlangen-Nuremberg, Maximiliansplatz 1, 91054 Erlangen, Germany
[5]Department of Internal Medicine III, University of Erlangen-Nuremberg, Krankenhausstr. 12, 91054 Erlangen, Germany
[†]Author for correspondence:
Tel.: +43 140 400 6467
Fax: +43 140 400 6475
welsch@bwh.harvard.edu

Advanced MRI in rheumatoid arthritis

MRI is now more intensively used to characterize the burden of inflammation and structural changes in the joint of patients with rheumatoid arthritis (RA). Owing to its strength in visualizing inflammatory tissue, MRI has been recognized as an excellent tool to define the quantity and quality of synovial inflammation in RA, in particular when visualizing the degree of synovitis outside the cortical bone shell and the presence of osteitis in the bone marrow of RA patients. Significant advances have been made in characterizing, quantifying and standardizing the specific morphological changes in RA patients due to observations made using MRI scans. Concerning bony irregularities, MRI depicts calcified bone as a signal void, comparably to radiography. Delineating cortical and trabecular bone with MRI is still limited by spatial resolution, as these are small structures in the small finger joints, and they contrast with adjacent tissues, particularly short transverse relaxation time (T2) tissues, such as ligaments and other fibrous structures. MRI nevertheless still delineates bone contours nicely, owing to its tomographic viewing perspective and the high contrast between fatty bone marrow and other tissues with higher free-water fibrous content. Furthermore, there is a high sensitivity for depicting inflammatory changes, such as bone marrow edema. Recent data have also underlined the importance of MRI in predicting a severe disease course of RA patients by demonstrating that MRI changes precede bone structure changes depicted by conventional radiography.

Structural damage in RA is based on an accumulation of bone erosion as well as cartilage degradation in the inflamed joints. MRI and high-resolution ultrasound have significantly improved our insight into the structural nature of bone erosion in RA. By contrast, direct visualization of cartilage degradation in RA is far less established and particularly difficult owing to the small cartilage volume in the small joints. Structural damage of articular cartilage is highlighted by radiographic joint space narrowing. MRI can visualize morphological alterations within the articular cartilage such as reduction in cartilage volume, cartilage contour irregularities, fissures and cartilage thinning [1–3]. As structural cartilage damage is preceded by biochemical alterations such as proteoglycan loss, there is a substantial interest in detecting such changes early in the course of the disease [4].

The biochemical MRI techniques most often reported to visualize cartilage ultrastructure are delayed gadolinium-enhanced MRI of cartilage (dGEMRIC) and T2 mapping [5–8]. Using dGEMRIC, biochemical MRI has the ability to quantify functionally relevant macromolecules within articular cartilage such as glycosamnioglycans (GAGs) [5]. GAGs are the main source of fixed charge density (FCD) in cartilage, which are often decreased in the early stages of cartilage degeneration [9] and are considered as a key factor in the progression of cartilage

future medicine part of fsg

damage in RA [10]. T2 relaxation time mapping reflects the interaction of water and the extracellular matrix. Changes in hydration as well as collagen anisotropy are reported to be early indicators of cartilage deterioration and can be visualized by T2 relaxation time mapping [6].

These recent advances in magnetic resonance (MR) sequences together with the implementation of high-resolution MRI due to high-field MR systems as well as sophisticated coil technology [8] have overcome existing limitations and led to promising *in vivo* approaches in morphological [11,12] and biochemical [13] MRI of the thin cartilage layer in the metacarpophalangeal (MCP) or the carpometacarpal (CMC) joint.

The aim of this article is to review the current literature and present the ideas of our working group on MRI of RA patients with the focus on cartilage imaging, and to demonstrate possible pathways and ideas in advanced morphological and biochemical MR cartilage imaging techniques. Although only few data are available on cartilage imaging in small finger joints in RA, this article intends to demonstrate – together with basic morphological imaging techniques as well as optimized dynamic MRI – the feasibility of biochemical MR techniques.

Morphological MRI in RA – again mainly based in cartilage imaging – will be discussed using conventional 2D and advanced 3D techniques. Furthermore, biochemical MRI techniques and their possible impact in RA will be elucidated.

As this article is based on cartilage imaging, most of the reviewed MR techniques base their experience in the knee joint and in osteoarthritis (OA) or cartilage repair. However, in RA the small finger joints are most commonly affected. Hence the present article tries to provide knowledge on cartilage MRI in general (based on the knee joint) and tries to transfer this knowledge to the small finger joints affected in RA.

Morphological MRI: initial experiences in RA

In RA, imaging techniques have played an important role in assessing disease progression and treatment response. Plain radiographs have been widely used to quantify disease progression; however, only relatively late signs of joint deterioration, such as joint space narrowing and bone erosion, can by detected by this method. MRI can visualize the bone and soft tissue in 3D and has the potential to measure inflammatory activity and joint destruction [14]. Exemplary coronal and axial morhological MRI is provided in Figure 1. These alterations, such as bone synovitis, bone marrow edema (osteitis) and bone erosion, can be imaged in different joints and assessed by the RA MRI Scoring (RAMRIS) system introduced by the Outcome Measures in RA Clinical Trials (OMERACT) group. This semiquantitative imaging score is widely used and, is shown to be suitable and reproducible in different studies [15–21]. In a recent review article, the key frontiers of MRI in RA are stated as: the measurement of the synovial volume, bone marrow edema and erosion predicting structural damage in RA; the dynamic MRI measurements to assess the inflammatory activity; and the challenges in the direct evaluation of articular cartilage, especially in the small joints [14].

In a recent study the effects of denosumab on structural damage in patients with RA were studied, where the primary end point was the longitudinal change as assessed by MRI erosion scoring [22]. At 6 months, the increase in the MRI erosion score from baseline was lower in the 60-mg denosumab group (mean change: 0.13; $p = 0.118$) and was significantly lower in the 180-mg denosumab group (mean change: 0.06; $p = 0.007$) compared with the placebo group (mean change: 1.75) [22]. This study provided the ability of MRI to serve in a longitudinal study as a primary end point.

MRI, with its excellent soft tissue contrast, has been shown to be superior in the detection of cartilage abnormalities [23–28]. Nevertheless, the use of cartilage-sensitive MRI techniques in RA is limited. In the peripheral small joints affected by RA such as the wrist, the MCP and proximal interphalangeal joints, the potential of cartilage imaging is still restricted owing to the thin cartilage layers and the lack of widely available high-field MR systems and dedicated, multichannel coil options.

In a very recent article on the development of anMRI-based cartilage scoring system for the use in RA, wrist joints were scored for cartilage narrowing [29]. Cartilage scores were higher in the established RA group (mean: 11.9) than in the early-stage RA group (mean: 2.15; $p < 0.001$). Although early-stage RA scores did not differ from healthy controls (mean: 2.3), cartilage scores correlated with synovitis ($r = 0.52$), bone edema ($r = 0.63$) and erosion scores ($r = 0.66$; $p < 0.001$). This study depicts the importance of the evaluation of articular cartilage in RA.

The signal, image quality and reproducibility, as well as the diagnostic validity, have been studied along different field strengths. Concerning the RAMRIS system, MRI image quality is superior

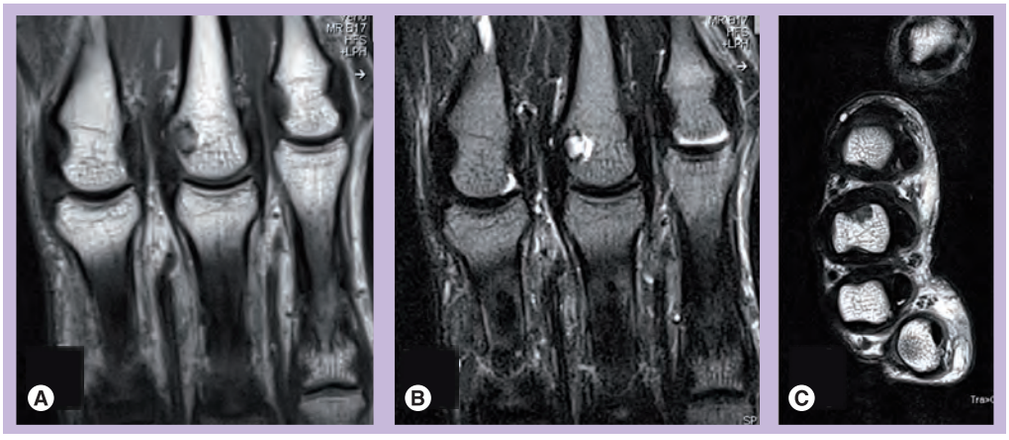

Figure 1. Standard morphological MRI. Coronal **(A)** proton density turbo spin echo and **(B)** short tau inversion recovery sequences of a 28-year-old patient with rheumatoid arthritis in remission. Metacarpophalangeal joints 2–4 are visualized by the use of a small, flexible coil. **(C)** Axial proton density turbo spin echo sequence detecting bony alterations distal to the metacarpophalangeal 3 joint.

at 3.0 Tesla. While an acceptable image quality is achieved at 1.5 Tesla, the evaluation of bone edema, synovitis and identification of small bone erosions could be improved by 3.0-Tesla MRI [30]. For example, the image quality of T1-weighted images was rated 14–22% better at 3.0 Tesla compared with 1.5 Tesla. Furthermore, inter- and intra-reader correlations, as another sign of image quality, were higher (up to 0.9 Telsa) at 3.0 Tesla compared with 1.5 Tesla with values ranging only up to 0.8 Telsa. Concerning cartilage imaging in the wrist, Saupe *et al.* compared the visibility and the contrast-to-noise ratio (CNR) of cartilage between 1.5- and 3.0-Tesla MRI scanners [31]. As expected, CNR between bone and cartilage was significantly higher for 3.0-Tesla MRI, ranging between a factor of 1.6 and 2.6 when comparing 3.0 Tesla and 1.5 Tesla. Comparably the qualitative analysis revealed superior results for 3.0-Tesla MRI. Nevertheless low-field extremity MRI might also play a role in future approaches and the evaluation of small finger joints in RA patients. So far, comparable results to 1.5-Telsa whole-body systems could be reached [32]. Furthermore, a comparison between conventional high-field MRI (1.5 Tesla) and 0.2-Tesla low-field-strength extremity MRI demonstrated no significant difference in the detection of bone erosions, synovitis and joint space narrowing between both MR techniques [33].

Nevertheless, cartilage lesions are not routinely assessed and diagnosed in the hand joints despite their clinical importance [34,35]. The preliminary results of Saupe *et al.* with 3.0-Tesla MRI of the wrist suggest that fat-saturated intermediate-weighted sequences allow good visualization of the radiocarpal and parts of the intercarpal cartilage [31]. Uhl *et al.* examined a fat-suppressed (FS) 3D fast low-angle shot (FLASH) sequence, a FS 3D fast imaging with steady-state precession (FISP), a FS 2D fast spin-echo (FSE) T2-weighted, and a 2D FS spin-echo T1-weighted sequence in their accuracy of detecting cartilage destruction in small joints of patients with RA [36]. This study demonstrated that 3D gradient-echo (GRE) sequences with fat suppression were best for imaging and grading of cartilage lesions in the small joints of RA patients.

As mentioned previously, one of the most important points in high-resolution MRI of the small finger joints, and especially the cartilage layers, is the coil selection. There are very promising results available on the use of dedicated wrist coils [29]. Nevertheless, the small finger joints are not usually covered by the wrist coils. A very interesting study of Yoshioka and co-workers compared two microscopy coils (47 and 23 mm in diameter) and small surface coil (diameter of 80 mm in diameter) in their evaluation of the triangular fibrocartilage complex [37]. In this study both microscopy coils demonstrated significantly higher signal-to-noise ratio (SNR) values than the conventional surface coil ($p < 0.05$ to $p < 0.001$). Furthermore, the subjective quality was significantly higher, ranging from 2.0 to 2.9 for the surface coil and from 2.2 to 4.0 for the microscopy coils on a scale where 4.0 represents the highest possible quality. The conspicuity of cartilage injury was then evaluated again by Yoshioka at 1.5 Tesla [38]. The evaluation of the benefits of 3.0 Tesla and a small surface coil (comparing 2D vs 3D) for assessing the wrist and hand joints and joint components was also performed with promising results [39].

Morphological cartilage MRI: basics

Experience of morphological MRI of the cartilage is still largely based on OA and cartilage repair of the knee joint. Nevertheless, most techniques can be used in the small joints of patients with RA. The most widely used MRI techniques are intermediate-weighted FSE and 3D FS GRE acquisition [3,40–43]. Whereas the GRE sequence visualizes cartilage defects attributable to T1 differences between cartilage and fluid, the FSE sequence uses differences in T2 weighting. Compared with fluid, cartilage is higher in signal intensity on FS T1-weighting and lower on intermediate or T2-weighting. While the 3D GRE sequence with fat suppression is suitable for visualization of the thickness and surface of cartilage and allows 3D volume measurements, the FSE sequence is sensitive for assessment of the internal cartilage structure as well [40–42]. The subchondral bone also displays high signal intensity, owing to fatty bone marrow, which remains relatively hyperintense on FSE T2 sequences. Matrix alterations in the cartilage as well as surface changes and fibrillation can thus be assessed. Another advantage of FSE sequences is their low sensitivity to magnetic susceptibility artefacts, which are suppressed by the multiple refocusing 180° pulses of the FSE, facilitating reliable postoperative MRI assessment. Both sequences, the FS 3D GRE and the T2-weighted FSE, have demonstrated excellent results with high sensitivity, specificity and accuracy for detecting cartilage lesions in the knee joint [40,42,44].

The potential of 3D sequences has been demonstrated in patients with RA. In an older feasibility study, a fat-saturated spoiled GRE (SPGR) sequence was used to assess the cartilage volume in the MCP joints [3]. The accuracy of cartilage volume measurements as assessed using MRI could be evaluated using cadaver joints as a gold standard. The measured accuracy errors were relatively low with -1.8% for the metacarpal cartilage and 9.1% for the proximal phalangeal cartilage [3].

Morphological cartilage MRI: advanced 3D

New 3D sequences have the potential of high-resolution isotropic imaging with a voxel size down to 0.3 mm^3 and can thus be reformatted in arbitrary planes. Although there are no data available in the literature so far, these isotropic sequences in the future may provide the potential to assess not only the cartilage surface within different small joints, but also the adjacent structures and pathologies mentioned previously, such as synovitis, bone marrow edema and bone erosion within a single sequence. The sequences are usually GRE based and termed FLASH or FISP (see above), SPGR, volume interpolated breath-hold examination, double-echo steady-state (DESS) and steady-state free precession (SSFP). Furthermore, recently available isotropic 3D FSE sequences called 'proton density sampling perfection with application optimized contrasts using different flip angle evolutions' or '3D FSE extended echo-train acquisition' may extend the spectrum of sequences. **Figure 2** provides an example of a new isotropic 3D FSE sequence and its possible multiplanar reconstruction, whereas an approach of ultrahigh in-plane resolution to visualize both cartilage layers in an MCP joint is provided in **Figure 3**.

A commonly implemented isotropic 3D sequence for cartilage imaging is the FLASH sequence, a FS gradient-recalled-echo sequence with radio-frequency spoiling [45]. This FS 3D-FLASH sequence demonstrates high CNR and high reproducibility in the segmentation of articular cartilage and facilitates accurate evaluation of total cartilage volume and regional distribution [46,47]. Hence, cartilage segmentation measurements could be established for quantitative MR evaluation and parameters such as cartilage thickness and volume have been suggested as sensitive image-based parameters for detecting and monitoring cartilage damage in OA [48]. The FLASH sequence has also been used to assess the cartilage volume over time in patients with RA [49]. It remains questionable if cartilage segmentation will be feasible in the small finger; however, in the longitudinal follow-up quantitative morphological MR techniques would be desirable.

Besides the well-established 3D-FLASH sequence, the 3D-DESS sequence was introduced as adequate MRI acquisition to measure changes of cartilage thickness and volume in a longitudinal follow-up study in patients with OA [50]. Although no studies are available on its use on small joints in RA patients, the value of the 3D DESS sequence will be of interest in future approaches of imaging small joints affected by RA. For imaging of the femuro-tibial joint by 3.0-Tesla MRI scanners the DESS sequence (precision error: 2.4–6.2%) yielded slightly superior results compared with the FLASH sequence (precision error: 3.0–6.4%) and permitted accurate and precise analysis of cartilage morphology [51]. Furthermore, a high

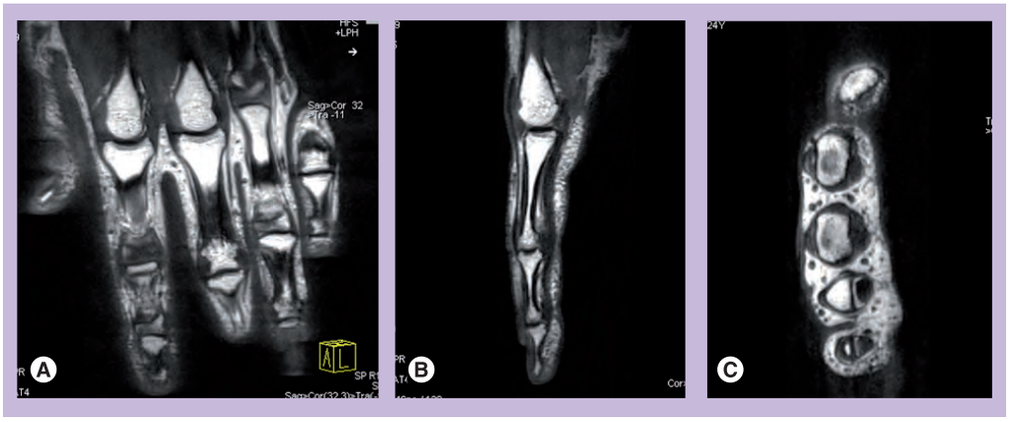

Figure 2. Isotropic 3D morphological MRI. A left forehand is visualized by the **(A)** coronal, **(B)** sagittal and **(C)** axial reformatiation of an isotropic (0.5 × 0.5 × 0.5 mm) 3D 'proton density sampling perfection with application optimized contrasts using different flip angle evolutions' sequence. Using the multiplanar reconstruction options, the complete forehand can be diagnosed.

correlation between both sequences, ranging form 0.88 to 1.0, could be assessed as an indication that both sequences can be used in the quantitative assessment of articular cartilage.

Furthermore, GRE-type sequences such as 3D-SPGR, FLASH, 3-point Dixon and DESS are well suited for depicting the cartilage volume, and thus, they are the sequence of choice for quantitative (volumetric) analysis of cartilage [23,52]. However, GRE-type sequences are less suited than fluid-sensitive sequences such as fat suppression intermediate (IM)-weighted, proton density (PD)-weighted or T2-weighted FSE sequences for depiction of subtle cartilage abnormalities [53,54]. With fat suppression IM-, PD- and T2- weighted FSE sequences, normal hyaline cartilage has intermediate signal intensity, and intra-articular fluid is bright, allowing good contrast owing to an 'arthrographic' effect to identify surface abnormalities as well as pathologies of cartilage matrix [55]. Moreover, GRE-type sequences are very susceptible to artifacts (motion artifacts from long imaging time and also susceptibility artifacts), leading to difficulty differentiating between true cartilage defect and signal changes owing to artefact [56].

Another 3D sequence with substantially higher SNR and CNR compared with the 3D-FLASH sequence is the 3D-True-FISP sequence [57]. This advantage in signal might allow higher spatial resolution and therefore potential improvement of the accuracy of the segmentation process, especially at the articular surface [57]. At high-field MRI this advantage might also be used to perform isotropic MR measurements in a minimal amount of time at a high resolution, as needed for the assessment of the small finger joints. Comparing the performance of a 3D-SPGR and two 3D-SSFP sequences at 1.5 and 3.0 Telsa, Kornaat *et al.* found SSFP-based techniques to show the highest increase in SNR and CNR using 3.0-Telsa MRI [58]. Hence for 3D-SPGR, CNR efficiencies between cartilage and its surrounding tissue increased compared with those at 1.5 Telsa by a factor of 2.12 (range: 1.75–2.47), for fat-saturated-SSFP by a factor of 2.11 (range: 1.58–2.80) and for Dixon SSFP by a factor of 2.39 (range: 2.09–2.83). In recent articles by Duc *et al.* a SSFP-based sequence (True-FISP) studied in detail at 1.5 Telsa also demonstrates promising

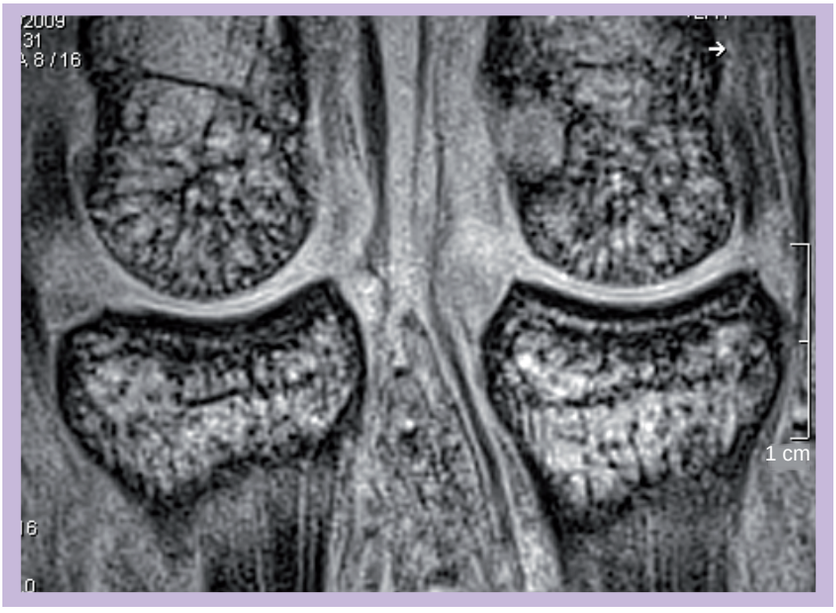

Figure 3. Ultrahigh in-plane resolution of the metacarpophalangeal joint. The same patient compared with FIGURES 1 & 2 is imaged using an ultrahigh-resolution (0.19 × 0.19 × 1.5 mm) T1 VIBE sequence based on an approach with two loop coils covering the metacarpophalangeal 2 and 3 joints. The cartilage can be differentiated and even the joint space is visible.

results. In comparison to a 3D-FLASH and a 3D-DESS sequence, the detection of cartilage defects is possible with similar sensitivity, specificity and accuracy for this water excitation SSFP sequence and shows the highest SNR and CNR efficiency [59–61].

Promising results in the assessment of cartilage lesions together with other pathologies might be provided by 3D FSE sequences. In a comparison to 2D FSE sequences, an isotropic (0.7 mm^3) 3D-FSE extended echo-train acquisition sequence showed isotropic data sets with the possibility of reformatting in arbitrary planes and high cartilage SNR [62]. Comparably, the 3D PD-SPACE sequence demonstrating very encouraging results in initial studies [63] needs to be optimized, for its use in the small hand joints. The potential of these sequences lies in the 3D assessment of the articular cartilage, the precise description of every plane, as well as the diagnosis of adjacent structures. A strong advantage of isotropic 3D data is to use them as a high-resolution 3D localizer for further evaluations, such as biochemical sequences which require a relatively large thickness slice to enable high in-plane resolution with sufficient SNR. Hence, in small hand joints biochemical evaluations can also be performed with an opportunity to gain good results by compositional MRI in difficult anatomic regions.

In a very recent study, the assessment of cartilage loss at the wrist in RA is provided by a newly introduced MRI scoring system based on 3.0-Telsa MRI and a dedicated wrist coil [29]. Using an optimal hardware setup, excellent and reproducible results could be achieved with high inter- and intraobserver reliability and intraclass correlations between 0.86 and 1.00. Furthermore, the results of this cartilage scoring system demonstrated significant correlations with synovitis (r = 0.52), bone edema (r = 0.63) and erosion (r = 0.66).

Biochemical cartilage MRI: initial experiences in RA

In addition to the morphologic assessment of cartilage structures a further major advance with MRI is the ability to image and quantify functionally relevant macromolecules within the articular cartilage (Figure 4). The most widely available techniques are dGEMRIC and T2 mapping [64]. Nevertheless, other techniques such as T1rho, T2* mapping, diffusion-weighted imaging (DWI), magnetization transfer or ultra-short echo-time (UTE) imaging have also shown their potential in the noninvasive evaluation of cartilage composition. These biochemical methodologies are commonly utilized to assess articular cartilage in patients with OA or in patients after cartilage repair procedures [5,8,65–68]. The development of these nondestructive imaging methods for evaluating the biochemical state of cartilage may have the potential to improve the understanding of the dynamics of cartilage degradation and in evaluating therapeutic efficacy.

For the visualization of proteoglycans, dGEMRIC has gained significant importance. The value of this technique in articular cartilage and the possible clinical applications have mainly been reported in the knee joint [5,69,70]. In patients with OA, reduced T1 values have been described as an early sign of cartilage degeneration based on a decreased proteoglycan content, visualizing preradiographic changes in the cartilage [66]. Similar results have been obtained by analyzing the cartilage of the hip joint [71]. A recent study demonstrated the feasibility of dGEMRIC in the first CMC joint at 1.5 Tesla using a 1-inch surface coil in a small group of OA patients [13], hence its usefulness in thinner cartilage layers has also been documented.

Besides the reported decrease of proteoglycans, an increase in water content and changes in the collagen network are early changes of the cartilage in RA [72]. The loss of proteoglycans reduces the binding of water and increases the cartilage permeability. Accordingly, the collagen matrix has to carry more load, resulting in geometrical changes of the collagen. These biochemical changes can be quantified by T2 mapping. The feasibility of T2 mapping has been proven in interphalangeal joints in healthy subjects [73]. Furthermore, initial results on the application of T2 mapping in the knee cartilage of RA patients demonstrate an increase in T2 relaxation times, reflecting microstructural differences [72]. Hence, quantitative T2 mapping might also be able to assess articular cartilage in small finger joints of patients with RA.

Other biochemical MRI techniques have been employed, mainly in the knee cartilage, although some have also investigated the ankle joint with its thinner cartilage using DWI, T2, or T2* mapping [74]. In RA, DWI, which exploits the translational motion of water protons [75,76], might have especially high potential. In recent studies, a relatively fast SSFP approach, based on a reversed FISP (PSIF) sequence, demonstrated promising results for the evaluation of cartilage repair [77,78]. The theoretical model of diffusion contributing to a steady-state signal

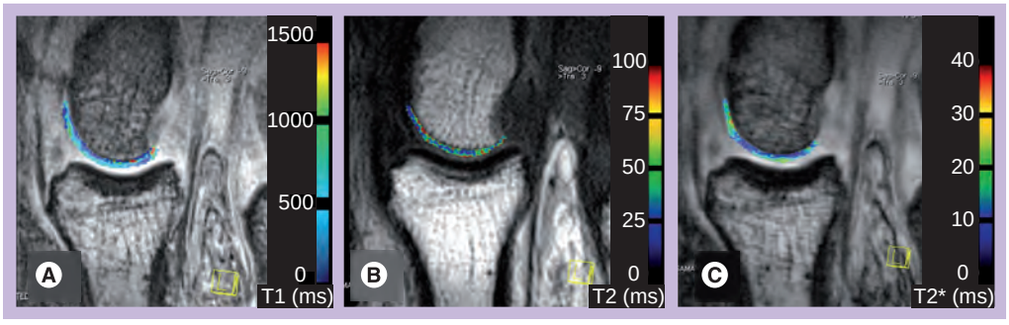

Figure 4. Ultrahigh-resolution coronal MRI of a metacarpophalangeal joint 2 from a 34-year-old female patient with seropositive rheumatoid arthritis. The cartilage layer is visualized using biochemical T1 delayed gadolinium-enhanced MRI of cartilage (dGEMRIC), biochemical multiecho spin-echo T2 mapping, and biochemical multiecho gradient echo T2* mapping. The overlaid quantitative **(A)** T1dGEMRIC, **(B)** T2 and **(C)** T2* images demonstrate the feasibility of T1 and T2 mapping techniques in the small finger joints.

was described several years ago [79]. However, by contrast to the basic Stejskal-Tanner diffusion acquisition model of DWI, which uses two gradient pulses in spin-echo-based sequences, the signal dependence of 3D-PSIF has a complex dependence on the flip angle α, T1, T2, TR and

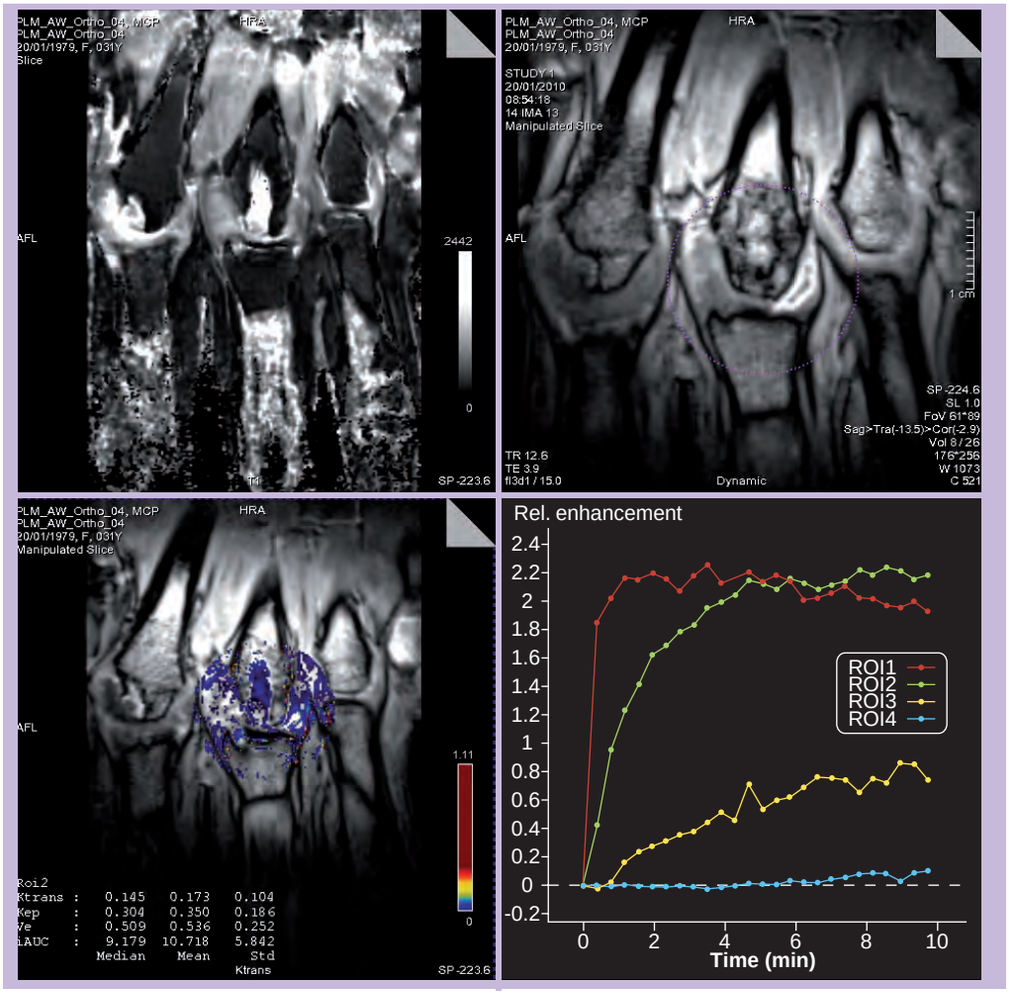

Figure 5. Dynamic analysis of a 50-year-old female patient with active rheumatoid arthritis based on a T1 fast low-angle shot sequence. The 3D analysis in the lower right window shows the analysis over time. The red curve represents the synovial, the green curve the synovialis, the yellow curve a pathologic subchondral bone formation and the blue line solid bone.
Rel.: Relative; ROI: Region of interest.

the single diffusion-sensitizing gradient, and is thus difficult to quantify. Nevertheless, a quantification of cartilage diffusion, as achieved by calculating apparent diffusion coefficient maps, is possible *in vivo*. With the availability of new sequence profiles and multichannel coils, DWI might be a useful tool to investigate the articular cartilage of small joints.

Comparably, high potential in RA might be provided by UTE. By contrast to musculoskeletal tissues with relatively long T2 relaxation components that can be visualized by conventional morphological and biochemical MRI techniques, tissues with short T2 components, such as deep and calcified cartilage layers, menisci and ligaments may profit from direct visualization by UTE [65]. UTE pulse sequences have echo times approximately 10- to 20-times shorter than the shortest times generally available for the clinical routine. Early degenerative changes in articular cartilage might be diagnosed earlier through visible changes in the calcified cartilage layer, which, to date, has been unexplored by MRI due to the short T2 components [65]. This approach might be especially interesting in RA, where the calcified cartilage layer and the subchondral bone plate are of the utmost importance in pathophysiological tracking of the disease.

Biochemical cartilage MRI: dGEMRIC

Of the major macromolecules, GAGs are important for the physiological function of the articular cartilage. GAGs are the main source of FCD in the cartilage, which are often decreased in the early stages of cartilage degeneration [9]. Intravenously administered gadolinium diethylenetriamine pentaacetate anion ($Gd\text{-}DTPA^{2-}$) penetrates into the cartilage through both the articular surface and the subchondral bone. The contrast equilibrates in inverse relation to the FCD, which is, in turn, directly related to the GAG concentration. Therefore, T1, which is determined by the $Gd\text{-}DTPA^{2-}$ concentration, becomes a specific measure of tissue GAG concentration, suggesting that $Gd\text{-}DTPA^{2-}$-enhanced MRI has the potential for monitoring GAG content of cartilage *in vivo* [80]. Thus, T1 mapping enhanced by delayed administration of $Gd\text{-}DTPA^{2-}$ (T1 dGEMRIC) can be considered the method of choice for detecting proteoglycan depletion in articular cartilage [66,81].

As the total scan time for dGEMRIC T1 mapping by standard inversion recovery (IR) evaluation is relatively long, a new approach for fast T1 mapping has demonstrated promising results and is increasing the clinical applicability of the dGEMRIC technique [70]. Since GAG content is responsible for cartilage function, particularly its tensile strength, the monitoring of the development of GAG content in RA may provide information about the quality of the cartilage and hence monitor degradation early. The applicability of this technique has also been shown in regions other than the knee joint [13,71,82]. A recent study facilitates dGEMRIC to assess the cartilage of the ankle joint, where the equilibrium seems to be reached after 30–45 min [83].Based on initial studies in small finger joints, 30 mins seem to be sufficient to reach this equilibrium and to monitor proteoglycan loss. In very recent studies, the feasibility of dGEMRIC in MCP joints in patients with RA has been demonstrated. Comparably to OA, lower dGEMRIC T1 values in cartilage of RA patients, compared with cartilage of healthy controls, indicates early proteoglycan loss in RA, although the morphological joint width is comparable to that of healthy subjects. dGEMRIC therefore seems to be feasible in small finger joints of RA patients and allows the monitoring and quantifying of GAG changes. Nevertheless in future studies, the optimal time-delay postinjection of $Gd\text{-}DTPA^{2-}$ has to be evaluated for T1 dGEMRIC imaging.

As the mapping of the GAG concentration is desirable for the diagnosis and monitoring of cartilage pathologies and the presented dGEMRIC technique has the limitation of contrast agent administration and a time delay before postcontrast MRI, a recently described technique for the assessment of GAG concentration *in vivo* by chemical exchange-dependent saturation transfer is of interest [84].

One very promising clinical application of dGEMRIC in RA patients was very recently presented by Tiderius *et al.* [85]. In seven patients with chronic RA and infliximab therapy, knee MRI was performed at baseline and after 7 months. However, a decrease in the dGEMRIC index from 382 ± 69 ms to 332 ± 85 ms, indicates an ongoing proteoglycan loss during therapy. These results still, however, have to be verified in larger cohorts and in the much more commonly involved small finger joints.

Biochemical cartilage MRI: T2 mapping

Probably the most frequently implemented biochemical MR technique is the transverse relaxation time (T2) of cartilage as a sensitive parameter for changes in water and collagen content and tissue anisotropy [6]. Cartilage

T2 reflects the interaction of water and the extracellular matrix on a molecular level. The collagen fiber orientation defines the layers of articular cartilage. Thus, the 3D organization and curvature of the collagen network, influenced by water mobility, the proteoglycan orientation and the resulting magic angle at 55° (with respect to the main magnetic field [B0]) influence the appearance of T2 [86,87]. In healthy articular cartilage, an increase in T2 values from deep to superficial cartilage layers can be observed based on the anisotropy of collagen fibers running perpendicular to the cortical bone in the deep layer of cartilage [88]. Histologically validated animal studies have shown this zonal increase in T2 values as a marker of hyaline or hyaline like cartilage structure after cartilage repair [89,90]. To visualize this zonal variation *in vivo*, high spatial resolution is essential. With a high enough SNR, this could be achieved at the high-field MRI. Although zonal T2 mapping is not yet possible in small finger joint of RA patients, it remains desirable for future approaches.

In OA T2 mapping has shown varying results [64,91,92]. An increase in T2 values is usually considered to represent the degradation of cartilage in OA as well as in RA; however, fibrocartilage (which might be a result of ongoing cartilage deterioration) is seen to provide lower T2 values compared with healthy cartilage [64,90,93]. This could limit the overall value of quantitative T2 mapping. Nevertheless, initial studies in the small finger joint of patients with RA also seem to demonstrate a clear increase in T2 values as a sign of cartilage infection, when comparing RA patients and healthy controls. Our own initial results of ongoing studies show that RA leads to a prolongation of T2 relaxation times of articular cartilage, which is in accordance with the findings on larger joints [72]. As the breakdown of collagen type II is a key aspect of cartilage damage in RA [94], T2 mapping might provide a quantitative measure for structural damage to the cartilage–collagen network. Hence, T2 mapping seems to offer potential in the area of RA, but extended studies will require sophisticated protocols together with an optimal coil design.

This latter aspect might be the crucial factor for all biochemical imaging techniques in the small finger joints of patients with RA. To assess the thin cartilage layers of these joints *in vivo* we therefore recommend that: the highest available field strength should be used; the best available coil selection should be made; optimization of the sequence protocol is essential; and optimal planning and slab selection should be carried out.

Conclusion

High-resolution 2D and 3D-MRI has the potential to detect subtle cartilage changes in the small finger joints of patients with RA. Complementary to morphological semiquantitative scoring systems such as RAMRIS, the evaluation of the articular cartilage should be taken into consideration when assessing joint degradation in RA. Essential requirements for high-resolution morphological as well as biochemical MRI of cartilage in small finger joints of patients with RA are nevertheless the availability of high-field MR systems and an optimal, dedicated coil selection. The biochemical techniques already feasible in RA, T1 dGEMRIC and T2 mapping provide complementary information to the morphological and dynamic MR approaches (**Figure 5**) in the small joints [3]. These techniques might allow for the early detection of cartilage changes providing an objective and quantitative method to monitor disease progression and the effects of anti-inflammatory drug therapies on cartilage damage.

Future perspective

High-field (3.0 Tesla) and ultrahigh-field (7.0 Tesla) MRI together with advanced coil technologies will, in the future, enable for high-resolution MRI of the whole hand, providing the possibility to score all small finger joints on a molecular level. Thus, functional imaging methods can visualize all structures within every joint, including the composition of the articular cartilage and can help to identify the course of disease in RA patients. Based on fully automatic segmentation algorithms, in future approaches this information could be used to quantify and follow-up different treatment options.

Financial & competing interests disclosure

Lars Lauer and Dominik Paul are employees of Siemens healthcare, Erlangen, Germany. The authors have no other relevant affiliations or financial involvement with any organization or entity with a financial interest in or financial conflict with the subject matter or materials discussed in the manuscript. This includes employment, consultancies, honoraria, stock ownership or options, expert testimony, grants or patents received or pending, or royalties.

No writing assistance was utilized in the production of this manuscript.

Executive summary

Advanced MRI in rheumatoid arthritis

- Direct visualization of cartilage degradation in rheumatoid arthritis (RA) is not yet established and particularly difficult owing to the small volume of cartilage in the small joints.
- MRI can visualize morphological alterations within the articular cartilage such as reduction in cartilage volume, cartilage contour irregularities, fissures and cartilage thinning.
- As structural cartilage damage is preceded by biochemical alterations, such as proteoglycan loss, there is a substantial interest in detecting such changes early in the course of disease before structural damage of the cartilage occurs.

Morphological MRI: initial experiences in RA

- Joint alterations in RA such as bone marrow edema, joint erosion and synovitis can be imaged in different joints and assessed by the RA MRI scoring system introduced by the Outcome Measures in RA Clinical Trials (OMERACT) group.
- In small joints, acceptable image quality can be achieved at 1.5 Tesla, but the exact evaluation of different pathologies, especially subtle cartilage changes, could be improved at 3.0 Tesla.

Morphological cartilage MRI: basics

- For volumetric evaluation of cartilage, gradient-echo-type sequences should be used.
- For subtle cartilage defect assessment, fat saturate fluid-sensitive spin-echo sequences (transverse relaxation time [T2] weighted, intermediate weighted or proton density weighted) should be used.

Morphological cartilage MRI: advanced 3D

- New 3D sequences have the potential of high-resolution isotropic imaging with a voxel size down to 0.3 mm^3 and can thus be reformatted in arbitrary planes.
- Promising results in the assessment of cartilage lesions together with other pathologies are provided by new isotropic 3D fast spin-echo sequences.

Biochemical cartilage MRI: initial experiences in RA

- On the basis of biochemical MRI it is possible to image the ultrastructure of articular cartilage.
- The most widely available techniques in biochemical cartilage imaging are gadolinium-enhanced MRI of cartilage (dGEMRIC) and T2 mapping, which are also feasible in the small finger joint of RA patients.

Biochemical cartilage MRI: dGEMRIC

- T1 dGEMRIC, which is determined by the gadolinium diethylenetriamine pentaacetate anion concentration, is a specific measure of tissue proteoglycan concentration.
- A new approach for fast T1 mapping has demonstrated promising results and is increasing the clinical applicability of the dGEMRIC technique.
- RA usually leads to reduced T1 dGEMRIC values of articular cartilage.
- Chemical exchange saturation transfer may become an alternative methodology in evaluating the proteoglycan concentration with the additional benefit of avoiding contrast agents.

Biochemical cartilage MRI: T2 mapping

- Cartilage T2 reflects the interaction of water and the extracellular matrix on a molecular level.
- RA usually leads to a prolongation of T2 relaxation times of articular cartilage.

Conclusion

- Morphological together with biochemical MRI and a dynamic, contrast-enhanced quantification of the joint inflammation provides objective and quantitative methods to monitoring disease progression and the effects of drug therapies on cartilage damage.

Bibliography

1 Peterfy CG: Magnetic resonance imaging in rheumatoid arthritis: current status and future directions. *J. Rheumatol.* 28(5), 1134–1142 (2001).

2 Gylys-Morin VM, Graham TB, Blebea JS *et al.*: Knee in early juvenile rheumatoid arthritis: MR imaging findings. *Radiology* 220(3), 696–706 (2001).

3 Peterfy CG, van Dijke CF, Lu Y *et al.*: Quantification of the volume of articular cartilage in the metacarpophalangeal joints of the hand: accuracy and precision of three-dimensional MR imaging. *Am. J. Roentgenol.* 165(2), 371–375 (1995).

4 Graham TB, Blebea JS, Gylys-Morin V, Passo MH: Magnetic resonance imaging in juvenile rheumatoid arthritis. *Semin. Arthritis Rheum.* 27(3), 161–168 (1997).

5 Burstein D, Velyvis J, Scott KT *et al.*: Protocol issues for delayed Gd(DTPA) (2-)-enhanced MRI: (dGEMRIC) for clinical evaluation of articular cartilage. *Magnet. Reson. Med.* 45(1), 36–41 (2001).

6 Mosher TJ, Dardzinski BJ: Cartilage MRI T2 relaxation time mapping: overview and applications. *Semin. Musculoskelet. Radiol.* 8(4), 355–368 (2004).

7 Potter HG, Black BR, Chong le R: New techniques in articular cartilage imaging. *Clin. Sports Med.* 28(1), 77–94 (2009).

8 Welsch GH, Mamisch TC, Hughes T, Domayer S, Marlovits S, Trattnig S: Advanced morphological and biochemical magnetic resonance imaging of cartilage repair procedures in the knee joint at 3 Tesla. *Semin. Musculoskelet. Radiol.* 12(3), 196–211 (2008).

9 Burstein D, Bashir A, Gray ML: MRI techniques in early stages of cartilage disease. *Invest. Radiol.* 35(10), 622–638 (2000).

10 Hollander AP, Atkins RM, Eastwood DM, Dieppe PA, Elson CJ: Human cartilage is degraded by rheumatoid arthritis synovial fluid but not by recombinant cytokines *in vitro*. *Clin. Exp. Immunol.* 83(1), 52–57 (1991).

11 Marzo-Ortega H, Tanner SF, Rhodes LA *et al.*: Magnetic resonance imaging in the assessment of metacarpophalangeal joint disease in early psoriatic and rheumatoid arthritis. *Scand. J. Rheumatol.* 38(2), 79–83 (2009).

12 Ostergaard M, Conaghan PG, O'Connor P *et al.*: Reducing invasiveness, duration, and cost of magnetic resonance imaging in rheumatoid arthritis by omitting intravenous contrast injection – does it change the assessment of inflammatory and destructive joint changes by the OMERACT RAMRIS? *J. Rheumatol.* 36(8), 1806–1810 (2009).

13 Williams A, Shetty SK, Burstein D, Day CS, McKenzie C: Delayed gadolinium enhanced MRI of cartilage (dGEMRIC) of the first carpometacarpal (1CMC) joint: a feasibility study. *Osteoarthritis Cartilage* 16(4), 530–532 (2008).

14 Hodgson RJ, O'Connor P, Moots R: MRI of rheumatoid arthritis image quantitation for the assessment of disease activity, progression and response to therapy. *Rheumatology (Oxford)* 47(1), 13–21 (2008).

15 Bird P, Ejbjerg B, McQueen F, Ostergaard M, Lassere M, Edmonds J: OMERACT Rheumatoid Arthritis Magnetic Resonance Imaging Studies. Exercise 5: an international multicenter reliability study using computerized MRI erosion volume measurements. *J. Rheumatol.* 30(6), 1380–1384 (2003).

16 Conaghan P, Edmonds J, Emery P *et al.*: Magnetic resonance imaging in rheumatoid arthritis: summary of OMERACT activities, current status, and plans. *J. Rheumatol.* 28(5), 1158–1162 (2001).

17 Conaghan P, Lassere M, Ostergaard M *et al.*: OMERACT Rheumatoid Arthritis Magnetic Resonance Imaging Studies. Exercise 4: an international multicenter longitudinal study using the RA-MRI Score. *J. Rheumatol.* 30(6), 1376–1379 (2003).

18 Lassere M, McQueen F, Ostergaard M *et al.*: OMERACT Rheumatoid Arthritis Magnetic Resonance Imaging Studies. Exercise 3: an international multicenter reliability study using the RA-MRI Score. *J. Rheumatol.* 30(6), 1366–1375 (2003).

19 McQueen F, Lassere M, Edmonds J *et al.*: OMERACT Rheumatoid Arthritis Magnetic Resonance Imaging Studies. Summary of OMERACT 6 MR Imaging Module. *J. Rheumatol.* 30(6), 1387–1392 (2003).

20 Ostergaard M, Peterfy C, Conaghan P *et al.*: OMERACT Rheumatoid Arthritis Magnetic Resonance Imaging Studies. Core set of MRI acquisitions, joint pathology definitions, and the OMERACT RA-MRI scoring system. *J. Rheumatol.* 30(6), 1385–1386 (2003).

21 Peterfy C, Edmonds J, Lassere M *et al.*: OMERACT rheumatoid arthritis MRI studies module. *J. Rheumatol.* 30(6), 1364–1365 (2003).

22 Cohen SB, Dore RK, Lane NE *et al.*: Denosumab treatment effects on structural damage, bone mineral density, and bone turnover in rheumatoid arthritis: a twelve-month, multicenter, randomized, double-blind, placebo-controlled, Phase II clinical trial. *Arthritis Rheum.* 58(5), 1299–1309 (2008).

23 Eckstein F, Burstein D, Link TM: Quantitative MRI of cartilage and bone: degenerative changes in osteoarthritis. *NMR Biomed.* 19(7), 822–854 (2006).

24 Gold GE, Burstein D, Dardzinski B, Lang P, Boada F, Mosher T: MRI of articular cartilage in OA: novel pulse sequences and compositional/functional markers. *Osteoarthritis Cartilage* 14(Suppl. A), A76–A86 (2006).

25 Recht M, White LM, Winalski CS, Miniaci A, Minas T, Parker RD: MR imaging of cartilage repair procedures. *Skeletal. Radiol.* 32(4), 185–200 (2003).

26 Recht MP, Goodwin DW, Winalski CS, White LM: MRI of articular cartilage: revisiting current status and future directions. *Am. J. Roentgenol.* 185(4), 899–914 (2005).

27 Trattnig S, Millington SA, Szomolanyi P, Marlovits S: MR imaging of osteochondral grafts and autologous chondrocyte implantation. *Eur. Radiol.* 17(1), 103–118 (2007).

28 Van Breuseghem I: Ultrastructural MR imaging techniques of the knee articular cartilage: problems for routine clinical application. *Eur. Radiol.* 14(2), 184–192 (2004).

29 McQueen F, Clarke A, McHaffie A *et al.*: Assessment of cartilage loss at the wrist in rheumatoid arthritis using a new MRI scoring system. *Ann. Rheum. Dis.* 69(11), 1971–1975 (2010).

30 Wieners G, Detert J, Streitparth F *et al.*: High-resolution MRI of the wrist and finger joints in patients with rheumatoid arthritis: comparison of 1.5 Tesla and 3.0 Tesla. *Eur. Radiol.* 17(8), 2176–2182 (2007).

31 Saupe N, Prussmann KP, Luechinger R, Bosiger P, Marincek B, Weishaupt D: MR imaging of the wrist: comparison between 1.5- and 3-T MR imaging – preliminary experience. *Radiology* 234(1), 256–264 (2005).

32 Suzuki T, Ito S, Handa S *et al.*: A new low-field extremity magnetic resonance imaging and proposed compact MRI score: evaluation of anti-tumor necrosis factor biologics on rheumatoid arthritis. *Mod. Rheumatol.* 19(4), 358–365 (2009).

33 Taouli B, Zaim S, Peterfy CG *et al.*: Rheumatoid arthritis of the hand and wrist: comparison of three imaging techniques. *Am. J. Roentgenol.* 182(4), 937–943 (2004).

34 Pfirrmann CW, Theumann NH, Botte MJ, Drape JL, Trudell DJ, Resnick D: MR imaging of the metacarpophalangeal joints of the fingers: part II. Detection of simulated injuries in cadavers. *Radiology* 222(2), 447–452 (2002).

35 Theumann NH, Pfirrmann CW, Drape JL, Trudell DJ, Resnick D: MR imaging of the metacarpophalangeal joints of the fingers: part I. Conventional MR imaging and MR arthrographic findings in cadavers. *Radiology* 222(2), 437–445 (2002).

36 Uhl M, Allmann KH, Ihling C, Hauer MP, Conca W, Langer M: Cartilage destruction in small joints by rheumatoid arthritis: assessment of fat-suppressed three-dimensional gradient-echo MR pulse sequences *in vitro*. *Skeletal Radiol.* 27(12), 677–682 (1998).

37 Yoshioka H, Ueno T, Tanaka T, Shindo M, Itai Y: High-resolution MR imaging of triangular fibrocartilage complex (TFCC), comparison of microscopy coils and a conventional small surface coil. *Skeletal Radiol.* 32(10), 575–581 (2003).

38 Yoshioka H, Tanaka T, Ueno T *et al.*: Study of ulnar variance with high-resolution MRI: correlation with triangular fibrocartilage complex and cartilage of ulnar side of wrist. *J. Magn. Reson. Imaging* 26(3), 714–719 (2007).

39 Bittersohl B, Huang T, Schneider E *et al.*: High-resolution MRI of the triangular fibrocartilage complex (TFCC) at 3T: comparison of surface coil and volume coil. *J. Magn. Reson. Imaging* 26(3), 701–707 (2007).

40 Disler DG, McCauley TR, Kelman CG *et al.*: Fat-suppressed three-dimensional spoiled gradient-echo MR imaging of hyaline cartilage defects in the knee: comparison with standard MR imaging and arthroscopy. *Am. J. Roentgenol.* 167(1), 127–132 (1996).

41 Potter HG, Linklater JM, Allen AA, Hannafin JA, Haas SB: Magnetic resonance imaging of articular cartilage in the knee. An evaluation with use of fast-spin-echo imaging. *J. Bone Joint Surg. Am.* 80(9), 1276–1284 (1998).

42 Recht M, Bobic V, Burstein D *et al.*: Magnetic resonance imaging of articular cartilage. *Clin. Orthop. Relat. Res.* (391 Suppl.), S379–S396 (2001).

43 Trattnig S, Huber M, Breitenseher MJ *et al.*: Imaging articular cartilage defects with 3D fat-suppressed echo planar imaging: comparison with conventional 3D fat-suppressed gradient echo sequence and correlation with histology. *J. Comput. Assist. Tomogr.* 22(1), 8–14 (1998).

44 Kramer J, Recht MP, Imhof H, Stiglbauer R, Engel A: Postcontrast MR arthrography in assessment of cartilage lesions. *J. Comput. Assist. Tomogr.* 18(2), 218–224 (1994).

45 Recht MP, Piraino DW, Paletta GA, Schils JP, Belhobek GH: Accuracy of fat-suppressed three-dimensional spoiled gradient-echo FLASH MR imaging in the detection of patellofemoral articular cartilage abnormalities. *Radiology* 198(1), 209–212 (1996).

46 Eckstein F, Sittek H, Milz S *et al.*: The potential of magnetic resonance imaging (MRI) for quantifying articular cartilage thickness – a methodological study. *Clin. Biomech. (Bristol, Avon)* 10(8), 434–440 (1995).

47 Eckstein F, Winzheimer M, Westhoff J *et al.*: Quantitative relationships of normal cartilage volumes of the human knee joint – assessment by magnetic resonance imaging. *Anat. Embryol.* 197(5), 383–390 (1998).

48 Gray ML, Eckstein F, Peterfy C, Dahlberg L, Kim YJ, Sorensen AG: Toward imaging biomarkers for osteoarthritis. *Clin. Orthop. Relat. Res.* (427 Suppl.), S175–S181 (2004).

49 Gandy SJ, Brett AD, Dieppe PA *et al.*: Measurement of cartilage volumes in rheumatoid arthritis using MRI. *Br. J. Radiol.* 78(925), 39–45 (2005).

50 Eckstein F, Kunz M, Schutzer M *et al.*: Two year longitudinal change and test-retest-precision of knee cartilage morphology in a pilot study for the osteoarthritis initiative. *Osteoarthritis Cartilage* 15(11), 1326–1332 (2007).

51 Eckstein F, Hudelmaier M, Wirth W *et al.*: Double echo steady state magnetic resonance imaging of knee articular cartilage at 3 Tesla: a pilot study for the osteoarthritis initiative. *Ann. Rheum. Dis.* 65(4), 433–441 (2006).

52 Bauer JS, Krause SJ, Ross CJ *et al.*: Volumetric cartilage measurements of porcine knee at 1.5-T and 3.0-T MR imaging: evaluation of precision and accuracy. *Radiology* 241(2), 399–406 (2006).

53 Barr C, Bauer JS, Malfair D *et al.*: MR imaging of the ankle at 3 Tesla and 1.5 Tesla: protocol optimization and application to cartilage, ligament and tendon pathology in cadaver specimens. *Eur. Radiol.* 17(6), 1518–1528 (2007).

54 Bauer JS, Barr C, Henning TD *et al.*: MR Imaging of the ankle at 3.0 Tesla and 1.5 Tesla in human cadaver specimens with artificially created lesions of cartilage and ligaments. *Invest. Radiol.* 43(9), 604–611 (2008).

55 Link TM: MR imaging in osteoarthritis: hardware, coils, and sequences. *Radiol. Clin. North Am.* 47(4), 617–632 (2009).

56 Hayashi D, Roemer FW, Guermazi A: Choice of pulse sequences for magnetic resonance imaging-based semiquantitative assessment of cartilage defects in osteoarthritis research: comment on the article by Dore *et al. Arthritis Rheum.* 62(12), 3830–3831 (2010).

57 Weckbach S, Mendlik T, Horger W, Wagner S, Reiser MF, Glaser C: Quantitative assessment of patellar cartilage volume and thickness at 3.0 tesla comparing a 3D-fast low angle shot versus a 3D-true fast imaging with steady-state precession sequence for reproducibility. *Invest. Radiol.* 41(2), 189–197 (2006).

58 Kornaat PR, Reeder SB, Koo S *et al.*: MR imaging of articular cartilage at 1.5T and 3.0T: comparison of SPGR and SSFP sequences. *Osteoarthritis Cartilage* 13(4), 338–344 (2005).

59 Duc SR, Koch P, Schmid MR, Horger W, Hodler J, Pfirrmann CW: Diagnosis of articular cartilage abnormalities of the knee: prospective clinical evaluation of a 3D water-excitation true FISP sequence. *Radiology* 243(2), 475–482 (2007).

60 Duc SR, Pfirrmann CW, Koch PP, Zanetti M, Hodler J: Internal knee derangement assessed with 3-minute 3-dimensional isovoxel true FISP MR sequence: preliminary study. *Radiology* 246(2), 526–535 (2008).

61 Duc SR, Pfirrmann CW, Schmid MR *et al.*: Articular cartilage defects detected with 3D water-excitation true FISP: prospective comparison with sequences commonly used for knee imaging. *Radiology* 245(1), 216–223 (2007).

62 Gold GE, Busse RF, Beehler C *et al.*: Isotropic MRI of the knee with 3D fast spin-echo extended echo-train acquisition (XETA), initial experience. *Am. J. Roentgenol.* 188(5), 1287–1293 (2007).

63 Notohamiprodjo M, Horng A, Pietschmann MF *et al.*: MRI of the knee at 3T: first clinical results with an isotropic PDfs-weighted 3D-TSE-sequence. *Invest. Radiol.* 44(9), 585–597 (2009).

64 Burstein D, Gray ML: Is MRI fulfilling its promise for molecular imaging of cartilage in arthritis? *Osteoarthritis Cartilage* 14(11), 1087–1090 (2006).

65 Du J, Takahashi AM, Chung CB: Ultrashort TE spectroscopic imaging (UTESI), application to the imaging of short T2 relaxation tissues in the musculoskeletal system. *J. Magn. Reson. Imaging* 29(2), 412–421 (2009).

66 Tiderius CJ, Olsson LE, Leander P, Ekberg O, Dahlberg L: Delayed gadolinium-enhanced MRI of cartilage (dGEMRIC) in early knee osteoarthritis. *Magnet. Reson. Med.* 49(3), 488–492 (2003).

67 Welsch GH, Mamisch TC, Marlovits S *et al.*: Quantitative T2 mapping during follow-up after matrix-associated autologous chondrocyte transplantation (MACT), full-thickness and zonal evaluation to visualize the maturation of cartilage repair tissue. *J. Orthop. Res.* 27(7), 957–963 (2009).

68 Welsch GH, Trattnig S, Scheffler K *et al.*: Magnetization transfer contrast and T2 mapping in the evaluation of cartilage repair tissue with 3T MRI. *J. Magn. Reson. Imaging* 28(4), 979–986 (2008).

69 Tiderius CJ, Olsson LE, de Verdier H, Leander P, Ekberg O, Dahlberg L: Gd-DTPA (2-)-enhanced MRI of femoral knee cartilage: a dose-response study in healthy volunteers. *Magnet. Reson. Med.* 46(6), 1067–1071 (2001).

70 Trattnig S, Marlovits S, Gebetsroither S *et al.*: Three-dimensional delayed gadolinium-enhanced MRI of cartilage (dGEMRIC) for *in vivo* evaluation of reparative cartilage after matrix-associated autologous chondrocyte transplantation at 3.0T: preliminary results. *J. Magn. Reson. Imaging* 26(4), 974–982 (2007).

71 Kim YJ, Jaramillo D, Millis MB, Gray ML, Burstein D: Assessment of early osteoarthritis in hip dysplasia with delayed gadolinium-enhanced magnetic resonance imaging of cartilage. *J. Bone Joint Surg. Am.* 85A(10), 1987–1992 (2003).

72 Kight AC, Dardzinski BJ, Laor T, Graham TB: Magnetic resonance imaging evaluation of the effects of juvenile rheumatoid arthritis on distal femoral weight-bearing cartilage. *Arthritis Rheum.* 50(3), 901–905 (2004).

73 Lazovic-Stojkovic J, Mosher TJ, Smith HE, Yang QX, Dardzinski BJ, Smith MB: Interphalangeal joint cartilage: high-spatial-resolution *in vivo* MR T2 mapping – a feasibility study. *Radiology* 233(1), 292–296 (2004).

74 Quirbach S, Trattnig S, Marlovits S *et al.*: Initial results of *in vivo* high-resolution morphological and biochemical cartilage imaging of patients after matrix-associated autologous chondrocyte transplantation (MACT) of the ankle. *Skeletal Radiol.* 38(8), 751–760 (2009).

75 Miller KL, Hargreaves BA, Gold GE, Pauly JM: Steady-state diffusion-weighted imaging of *in vivo* knee cartilage. *Magn. Reson. Med.* 51(2), 394–398 (2004).

76 Mlynarik V, Sulzbacher I, Bittsansky M, Fuiko R, Trattnig S: Investigation of apparent diffusion constant as an indicator of early degenerative disease in articular cartilage. *J. Magn. Reson. Imaging* 17(4), 440–444 (2003).

77 Friedrich KM, Mamisch TC, Plank C *et al.*: Diffusion-weighted imaging for the follow-up of patients after matrix-associated autologous chondrocyte transplantation. *Eur. J. Radiol.* 73(3), 622–628 (2010).

78 Mamisch TC, Menzel MI, Welsch GH *et al.*: Steady-state diffusion imaging for MR *in vivo* evaluation of reparative cartilage after matrix-associated autologous chondrocyte transplantation at 3 Tesla – preliminary results. *Eur. J. Radiol.* 65(1), 72–79 (2008).

79 Buxton RB: The diffusion sensitivity of fast steady-state free precession imaging. *Magn. Reson. Med.* 29(2), 235–243 (1993).

80 Bashir A, Gray ML, Boutin RD, Burstein D: Glycosaminoglycan in articular cartilage: *in vivo* assessment with delayed Gd(DTPA) (2-)-enhanced MR imaging. *Radiology* 205(2), 551–558 (1997).

81 Williams A, Gillis A, McKenzie C *et al.*: Glycosaminoglycan distribution in cartilage as determined by delayed gadolinium-enhanced MRI of cartilage (dGEMRIC), potential clinical applications. *Am. J. Roentgenol.* 182(1), 167–172 (2004).

82 Vaga S, Raimondi MT, Caiani EG *et al.*: Quantitative assessment of intervertebral disc glycosaminoglycan distribution by gadolinium-enhanced MRI in orthopedic patients. *Magn. Reson. Med.* 59(1), 85–95 (2008).

83 Domayer SE, Trattnig S, Stelzeneder D *et al.*: Delayed gadolinium-enhanced MRI of cartilage in the ankle at 3 T: feasibility and preliminary results after matrix-associated autologous chondrocyte implantation. *J. Magn. Reson. Imaging* 31(3), 732–739 (2010).

84 Ling W, Regatte RR, Navon G, Jerschow A: Assessment of glycosaminoglycan concentration *in vivo* by chemical exchange-dependent saturation transfer (gagCEST). *Proc. Natl Acad. Sci. USA* 105(7), 2266–2270 (2008).

85 Tiderius CJ, Sandin J, Svensson J, Dahlberg LE, Jacobsson L: Knee cartilage quality assessed with dGEMRIC in rheumatoid arthritis patients before and after treatment with a TNF inhibitor. *Acta Radiol.* 51(9), 1034–1037 (2010).

86 Goodwin DW, Wadghiri YZ, Dunn JF: Micro-imaging of articular cartilage: T2, proton density, and the magic angle effect. *Acad. Radiol.* 5(11), 790–798 (1998).

87 Goodwin DW, Zhu H, Dunn JF: *In vitro* MR imaging of hyaline cartilage: correlation with scanning electron microscopy. *Am. J. Roentgenol.* 174(2), 405–409 (2000).

88 Smith HE, Mosher TJ, Dardzinski BJ *et al.*: Spatial variation in cartilage T2 of the knee. *J. Magn. Reson. Imaging* 14(1), 50–55 (2001).

89 Watrin-Pinzano A, Ruaud JP, Cheli Y *et al.*: Evaluation of cartilage repair tissue after biomaterial implantation in rat patella by using T2 mapping. *MAGMA* 17(3–6), 219–228 (2004).

90 White LM, Sussman MS, Hurtig M, Probyn L, Tomlinson G, Kandel R: Cartilage T2 assessment: differentiation of normal hyaline cartilage and reparative tissue after arthroscopic cartilage repair in equine subjects. *Radiology* 241(2), 407–414 (2006).

91 David-Vaudey E, Ghosh S, Ries M, Majumdar S: T2 relaxation time measurements in osteoarthritis. *Magn. Reson. Imaging* 22(5), 673–682 (2004).

92 Dunn TC, Lu Y, Jin H, Ries MD, Majumdar S: T2 relaxation time of cartilage at MR imaging: comparison with severity of knee osteoarthritis. *Radiology* 232(2), 592–598 (2004).

93 Welsch GH, Mamisch TC, Domayer SE *et al.*: Cartilage T2 assessment at 3-T MR imaging: *in vivo* differentiation of normal hyaline cartilage from reparative tissue after two cartilage repair procedures – initial experience. *Radiology* 247(1), 154–161 (2008).

94 Nissim A, Winyard PG, Corrigall V *et al.*: Generation of neoantigenic epitopes after posttranslational modification of type II collagen by factors present within the inflamed joint. *Arthritis Rheum.* 52(12), 3829–3838 (2005).